Volume 157, June 2022

ISSN 1359-835X

composites

Part A: applied science and manufacturing

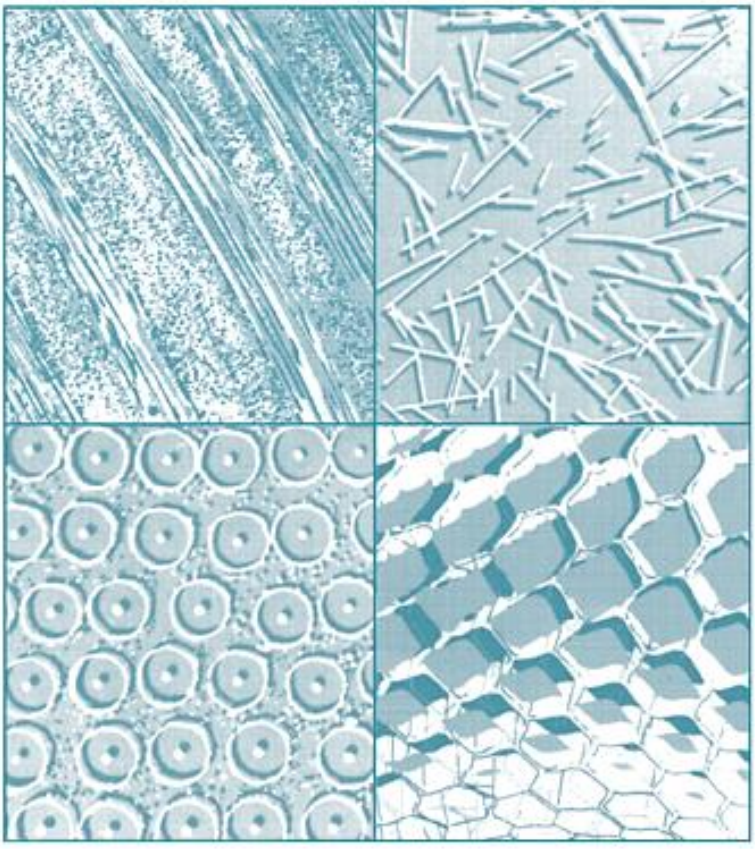

http://www.elsevier.com/locate/compositesa

Available online at www.sciencedirect.com

ScienceDirect

1. Full text access
   Editorial Board
   Article 106344
   Download PDF
2. select article Ultra-tough and in-situ repairable carbon/epoxy composite with EMAA
   Research articleAbstract only
   Ultra-tough and in-situ repairable carbon/epoxy composite with EMAA
   Thomas W. Loh, Raj B. Ladani, Adrian Orifici, Everson Kandare
   Article 106206
   Purchase PDF
   Article preview
3. select article Dynamic analysis of scarf adhesive joints in CFRP composites modified with Al₂O₃-nanoparticles under fatigue loading at different temperatures
   Research articleAbstract only
   Dynamic analysis of scarf adhesive joints in CFRP composites modified with Al_2O_3-nanoparticles under fatigue loading at different temperatures
   U.A. Khashaba
   Article 106277
   Purchase PDF
   Article preview
4. select article A novel method to fabricate two-dimensional nanomaterial based on electrospinning
   Research articleAbstract only
   A novel method to fabricate two-dimensional nanomaterial based on electrospinning
   Wenjing Ji, Guojie Zhao, Cong Guo, Li Fan, ... Qiang Fu
   Article 106275
   Purchase PDF
   Article preview
5. select article Electrospun porous carbon nanofibers @ SnO_x nanocomposites for high-performance supercapacitors: Microstructures and electrochemical properties
   Research articleAbstract only

Electrospun porous carbon nanofibers @ SnO_x nanocomposites for high-performance supercapacitors: Microstructures and electrochemical properties
Meilian Cao, Dong Wang, Jiqing Lu, Wanli Cheng, ... Jianbo Zhou
Article 106278
Purchase PDF
Article preview

6. select article Eddy current testing for estimation of anisotropic electrical conductivity of multidirectional carbon fiber reinforced plastic laminates
Research articleAbstract only
Eddy current testing for estimation of anisotropic electrical conductivity of multidirectional carbon fiber reinforced plastic laminates
Koichi Mizukami, Yudai Watanabe, Keiji Ogi
Article 106274
Purchase PDF
Article preview
7. select article Dynamic behavior of impact hardening elastomer: A flexible projectile material with unique rate-dependent performance
Research articleAbstract only
Dynamic behavior of impact hardening elastomer: A flexible projectile material with unique rate-dependent performance
Chunyu Zhao, Yu Wang, Mingyang Ni, Xiaokang He, ... Xinglong Gong
Article 106285
Purchase PDF
Article preview
8. select article Transversal friction of epoxy-lubricated and dry carbon tows: From initial stages to stabilised state
Research articleAbstract only
Transversal friction of epoxy-lubricated and dry carbon tows: From initial stages to stabilised state
Olga Smerdova, Omar Benchekroun, Noel Brunetiere
Article 106263
Purchase PDF
Article preview

9. select article Highly thermally conductive SiO₂-coated NFC/BNNS hybrid films with water resistance
   Research articleAbstract only
   Highly thermally conductive SiO_2-coated NFC/BNNS hybrid films with water resistance
   Na Song, Qi Wang, Dejin Jiao, Haidong Pan, ... Peng Ding
   Article 106261
   Purchase PDF
   Article preview
10. select article Tensile strength of CFRP with curvilinearly arranged carbon fiber along the principal stress direction fabricated by the electrodeposition resin molding
    Research articleAbstract only
    Tensile strength of CFRP with curvilinearly arranged carbon fiber along the principal stress direction fabricated by the electrodeposition resin molding
    Kazuaki Katagiri, Shinya Honda, Shota Nakaya, Takahiro Kimura, ... Katsuhiko Sasaki
    Article 106271
    Purchase PDF
    Article preview
11. select article Excellent thermally conducting modified graphite nanoplatelets and MWCNTs/poly(phenylene sulfone) composites for high-performance electromagnetic interference shielding effectiveness
    Research articleAbstract only
    Excellent thermally conducting modified graphite nanoplatelets and MWCNTs/poly(phenylene sulfone) composites for high-performance electromagnetic interference shielding effectiveness
    Qingxia He, Rui Chen, Shu Li, Zhenyang Wang, ... Jianxin Mu
    Article 106280
    Purchase PDF
    Article preview
12. select article An evaluation of the influence of manufacturing methods on interlocked aluminium-thermoplastic composite joint performance
    Research article*Open access*
    An evaluation of the influence of manufacturing methods on interlocked aluminium-thermoplastic composite joint performance

Karthik Ramaswamy, Ronan M. O'Higgins, John Lyons, Michael A. McCarthy, Conor T. McCarthy
Article 106281
Download PDF
Article preview

13. select article A modified 360° netting vein bionic structure for enhancing thermal properties of polymer/nanofiber/nanoparticle composite
Research articleAbstract only
A modified 360° netting vein bionic structure for enhancing thermal properties of polymer/nanofiber/nanoparticle composite
Yunna Sun, Yongjin Wu, Han Cai, Jiangbo Luo, ... Guifu Ding
Article 106276
Purchase PDF
Article preview

14. select article Biobased PLA/sugarcane bagasse fiber composites: Effect of fiber characteristics and interfacial adhesion on properties
Research article*Open access*
Biobased PLA/sugarcane bagasse fiber composites: Effect of fiber characteristics and interfacial adhesion on properties
András Bartos, Kristóf Nagy, Juliana Anggono, Antoni, ... Béla Pukánszky
Article 106273
Download PDF
Article preview

15. select article Constructing fibrillated skeleton with highly aligned boron nitride nanosheets confined in alumina fiber via electrospinning and sintering for thermally conductive composite
Research articleAbstract only
Constructing fibrillated skeleton with highly aligned boron nitride nanosheets confined in alumina fiber via electrospinning and sintering for thermally conductive composite
Li Fan, Shuai Zhang, Guojie Zhao, Qiang Fu
Article 106282
Purchase PDF
Article preview

16. select article PEG-filled kapok fiber/sodium alginate aerogel loaded phase change composite material with high thermal conductivity and excellent shape stability
Research articleAbstract only
PEG-filled kapok fiber/sodium alginate aerogel loaded phase change composite material with high thermal conductivity and excellent shape stability
Qiang Zhang, Bing Chen, Kun Wu, Bingfei Nan, ... Mangeng Lu
Article 106279
Purchase PDF
Article preview

17. select article Fabrication and applications of polyimide nano-aerogels
Research articleAbstract only
Fabrication and applications of polyimide nano-aerogels
Baolu Shi, Bin Ma, Chenqi Wang, Han He, ... Yanfei Chen
Article 106283
Purchase PDF
Article preview

18. select article 3D Graphene – sponge skeleton reinforced polysulfide rubber nanocomposites with improved electrical and thermal conductivity
Research articleAbstract only
3D Graphene – sponge skeleton reinforced polysulfide rubber nanocomposites with improved electrical and thermal conductivity
Wenjie Tao, Shaohua Zeng, Ying Xu, Wangyan Nie, ... Pengpeng Chen
Article 106293
Purchase PDF
Article preview

19. select article Flexible MXene-coated melamine foam based phase change material composites for integrated solar-thermal energy conversion/storage, shape memory and thermal therapy functions
Research articleAbstract only
Flexible MXene-coated melamine foam based phase change material composites for integrated solar-thermal energy conversion/storage, shape memory and thermal therapy functions

Yao-wen Shao, Wen-wen Hu, Meng-hang Gao, Yuan-yuan Xiao, ... Yong Wang
Article 106291
Purchase PDF
Article preview

20. select article Robust bioinspired MXene-based flexible films with excellent thermal conductivity and photothermal properties
Research articleAbstract only
Robust bioinspired MXene-based flexible films with excellent thermal conductivity and photothermal properties
Enxiang Jiao, Kun Wu, Yingchun Liu, Maoping Lu, ... Mangeng Lu
Article 106290
Purchase PDF
Article preview

21. select article Investigation on the compressive damage mechanisms of 3D woven composites considering stochastic fiber initial misalignment
Research articleAbstract only
Investigation on the compressive damage mechanisms of 3D woven composites considering stochastic fiber initial misalignment
Tao Zheng, Licheng Guo, Ruijian Sun, Zhixing Li, Hongjun Yu
Article 106295
Purchase PDF
Article preview

22. select article Automated braiding of non-axisymmetric structures using an iterative inverse solution with angle control
Research articleAbstract only
Automated braiding of non-axisymmetric structures using an iterative inverse solution with angle control
Marc Gondran, Yasmine Abdin, Yohan Gendreau, Farbod Khameneifar, Louis Laberge Lebel
Article 106288
Purchase PDF
Article preview

23. select article Processing temperature window design via controlling matrix composition for polypropylene-based self-reinforced composites
Research articleAbstract only

Processing temperature window design via controlling matrix composition for polypropylene-based self-reinforced composites
Hyeseong Lee, Yoon Sang Kim, Woo Hyuk Choi, Deok Woo Yun, ... Seong Yun Kim
Article 106301
Purchase PDF
Article preview

24. select article Three-point bending properties of carbon fiber/honeycomb sandwich panels with short-fiber tissue and carbon-fiber belt interfacial toughening at different loading rate
Research articleAbstract only
Three-point bending properties of carbon fiber/honeycomb sandwich panels with short-fiber tissue and carbon-fiber belt interfacial toughening at different loading rate
Zhi Sun, Hongjie Chen, Ziwen Song, Haoyang Liu, ... Shanshan Shi
Article 106289
Purchase PDF
Article preview

25. select article Consolidation-driven wrinkling in carbon/epoxy woven fabric prepregs: An experimental and numerical study
Research articleAbstract only
Consolidation-driven wrinkling in carbon/epoxy woven fabric prepregs: An experimental and numerical study
Armin Rashidi, Jonathan P.-H. Belnoue, Adam J. Thompson, Stephen R. Hallett, Abbas S. Milani
Article 106298
Purchase PDF
Article preview

26. select article Theoretical prediction of effective stiffness of nonwoven fibrous networks with straight and curved nanofibers
Research articleAbstract only
Theoretical prediction of effective stiffness of nonwoven fibrous networks with straight and curved nanofibers
Mang Zhang, Wenbin Lu, Pelagia Irene Gouma, Zhiping Xu, Lifeng Wang
Article 106311

Purchase PDF
Article preview

27. select article Lightweight multiscale hybrid carbon-quartz fiber fabric reinforced phenolic-silica aerogel nanocomposite for high temperature thermal protection
Research articleAbstract only
Lightweight multiscale hybrid carbon-quartz fiber fabric reinforced phenolic-silica aerogel nanocomposite for high temperature thermal protection
Haiming Cheng, Zihao Fan, Changqing Hong, Xinghong Zhang
Article 106313
Purchase PDF
Article preview

28. select article Conductive MXene/melamine sponge combined with 3D printing resin base prepared as an electromagnetic interferences shielding switch
Research articleAbstract only
Conductive MXene/melamine sponge combined with 3D printing resin base prepared as an electromagnetic interferences shielding switch
Wenjing Yuan, Haitao Liu, Xihua Wang, Li Huang, ... Ye Yuan
Article 106238
Purchase PDF
Article preview

29. select article Simulating the effect of fabric bending stiffness on the wrinkling behaviour of biaxial fabrics during preforming
Research articleAbstract only
Simulating the effect of fabric bending stiffness on the wrinkling behaviour of biaxial fabrics during preforming
F. Yu, S. Chen, L.T. Harper, N.A. Warrior
Article 106308
Purchase PDF
Article preview

30. select article Facile synthesis of a novel zinc-triazole complex for simultaneous improvement in fire safety and mechanical properties of epoxy resins
Research articleAbstract only

Facile synthesis of a novel zinc-triazole complex for simultaneous improvement in fire safety and mechanical properties of epoxy resins
Hafezeh Nabipour, Xin Wang, Lei Song, Yuan Hu
Article 106284
Purchase PDF
Article preview

31. select article Breathing-effect assisted transferring large-area PEDOT:PSS to PDMS substrate with robust adhesion for stable flexible pressure sensor
Research articleAbstract only
Breathing-effect assisted transferring large-area PEDOT:PSS to PDMS substrate with robust adhesion for stable flexible pressure sensor
Ziting Tan, Hongwei Li, Yinan Huang, Xue Gong, ... Wenping Hu
Article 106299
Purchase PDF
Article preview

32. select article Vibration attenuation of finite-size metaconcrete: Mechanism, prediction and verification
Research articleAbstract only
Vibration attenuation of finite-size metaconcrete: Mechanism, prediction and verification
Yang Liu, Xiyue An, Hailong Chen, Hualin Fan
Article 106294
Purchase PDF
Article preview

33. select article Understanding macroscopic assemblies of carbon nanostructures with microstructural complexity
Research articleAbstract only
Understanding macroscopic assemblies of carbon nanostructures with microstructural complexity
Shijun Wang, Jiahao Lin, Zhen Xu, Zhiping Xu
Article 106318
Purchase PDF
Article preview

34. select article Improving the effects of plasma polymerization on carbon fiber using a surface modification pretreatment
Research articleAbstract only

Improving the effects of plasma polymerization on carbon fiber using a surface modification pretreatment
Daniel J. Eyckens, Karyn Jarvis, Anders J. Barlow, Yanting Yin, ... Luke C. Henderson
Article 106319
Purchase PDF
Article preview

35. select article Moderation of thermoplastic composite crystallinity and mechanical properties through in situ manufacturing and post-manufacturing tempering: Part 1 – Mechanical characterisation
Research articleAbstract only
Moderation of thermoplastic composite crystallinity and mechanical properties through in situ manufacturing and post-manufacturing tempering: Part 1 – Mechanical characterisation
A.R. Chadwick, K. Kotzur, S. Nowotny
Article 106286
Purchase PDF
Article preview

36. select article Influence of the anisotropy of sisal fibers on the mechanical properties of high performance unidirectional biocomposite lamina and micromechanical models
Research articleAbstract only
Influence of the anisotropy of sisal fibers on the mechanical properties of high performance unidirectional biocomposite lamina and micromechanical models
Bernardo Zuccarello, Carmelo Militello, Francesco Bongiorno
Article 106320
Purchase PDF
Article preview

37. select article Selective distribution of SrTiO₃ in co-continuous composites: An effective method to improve the dielectric and mechanical properties
Research articleAbstract only
Selective distribution of $SrTiO_3$ in co-continuous composites: An effective method to improve the dielectric and mechanical properties
Zepeng Mao, Haoxuan Sun, Jun Zhang
Article 106312
Purchase PDF

Article preview

38. select article Effect of fiber misalignment on bending strength of pultruded hybrid polymer matrix composite rods subjected to bending and tension
Research articleAbstract only
Effect of fiber misalignment on bending strength of pultruded hybrid polymer matrix composite rods subjected to bending and tension
D.H. Waters, J.D. Hoffman, M. Kumosa
Article 106287
Purchase PDF
Article preview

39. select article Bayesian inversion algorithm for estimating local variations in permeability and porosity of reinforcements using experimental data
Research article*Open access*
Bayesian inversion algorithm for estimating local variations in permeability and porosity of reinforcements using experimental data
M.Y. Matveev, A. Endruweit, A.C. Long, M.A. Iglesias, M.V. Tretyakov
Article 106323
Download PDF
Article preview

40. select article Effect of nano-scale Cu particles on the electrical property of CNT/polymer nanocomposites
Research articleAbstract only
Effect of nano-scale Cu particles on the electrical property of CNT/polymer nanocomposites
Yang Wang, Xuhao Wang, Xinhui Cao, Shen Gong, ... Zhou Li
Article 106325
Purchase PDF
Article preview

41. select article A numerical approach to characterize the viscoelastic behaviour of fibre beds and to evaluate the influence of strain deviations on viscoelastic parameter extraction
Research article*Open access*
A numerical approach to characterize the viscoelastic behaviour of fibre beds and to evaluate the influence of strain deviations on viscoelastic parameter extraction
Vincent Werlen, Christian Rytka, Véronique Michaud

Article 106315
Download PDF
Article preview

42. select article Mechanical properties and failure mode of thin-ply fiber metal laminates under out-of-plane loading
Research articleAbstract only
Mechanical properties and failure mode of thin-ply fiber metal laminates under out-of-plane loading
Kohei Yamada, Benedikt Kötter, Masaaki Nishikawa, Shuto Fukudome, ... Masaki Hojo
Article 106267
Purchase PDF
Article preview

43. select article Numerical and experimental analysis of resin-flow, heat-transfer, and cure in a resin-injection pultrusion process
Research articleAbstract only
Numerical and experimental analysis of resin-flow, heat-transfer, and cure in a resin-injection pultrusion process
Michael Sandberg, Onur Yuksel, Ismet Baran, Jesper H. Hattel, Jon Spangenberg
Article 106231
Purchase PDF
Article preview

44. select article Computational simulation of the damage response for machining long fibre reinforced plastic (LFRP) composite parts: A review
Review articleAbstract only
Computational simulation of the damage response for machining long fibre reinforced plastic (LFRP) composite parts: A review
Xiaonan Wang, Fuji Wang, Tianyu Gu, Zhenyuan Jia, Yu Shi
Article 106296
Purchase PDF
Article preview

45. select article Progress in research on composite cryogenic propellant tank for large aerospace vehicles
Review articleAbstract only
Progress in research on composite cryogenic propellant tank for large aerospace vehicles
Ni Liu, Bin Ma, Feng Liu, Wenxuan Huang, ... Yazheng Yang

Article 106297
Purchase PDF
Article preview

46. select article Electrospun fibrous materials and their applications for electromagnetic interference shielding: A review
Review articleAbstract only
Electrospun fibrous materials and their applications for electromagnetic interference shielding: A review
Hongtao Guo, Yiming Chen, Yang Li, Wei Zhou, ... Shaohua Jiang
Article 106309
Purchase PDF
Article preview

47. select article Corrigendum to “Three-dimensional network constructed by vertically oriented multilayer graphene and SiC nanowires for improving thermal conductivity and operating safety of epoxy composites with ultralow loading” [Compos. Part A: Appl. Sci. Manuf. 139 (2020) 106062]
ErratumFull text access
Corrigendum to “Three-dimensional network constructed by vertically oriented multilayer graphene and SiC nanowires for improving thermal conductivity and operating safety of epoxy composites with ultralow loading” [Compos. Part A: Appl. Sci. Manuf. 139 (2020) 106062]
Jing He, Hua Wang, Qiqi Qu, Zheng Su, ... Xingyou Tian
Article 106324
Download PDF

composites

Part A: applied science and manufacturing

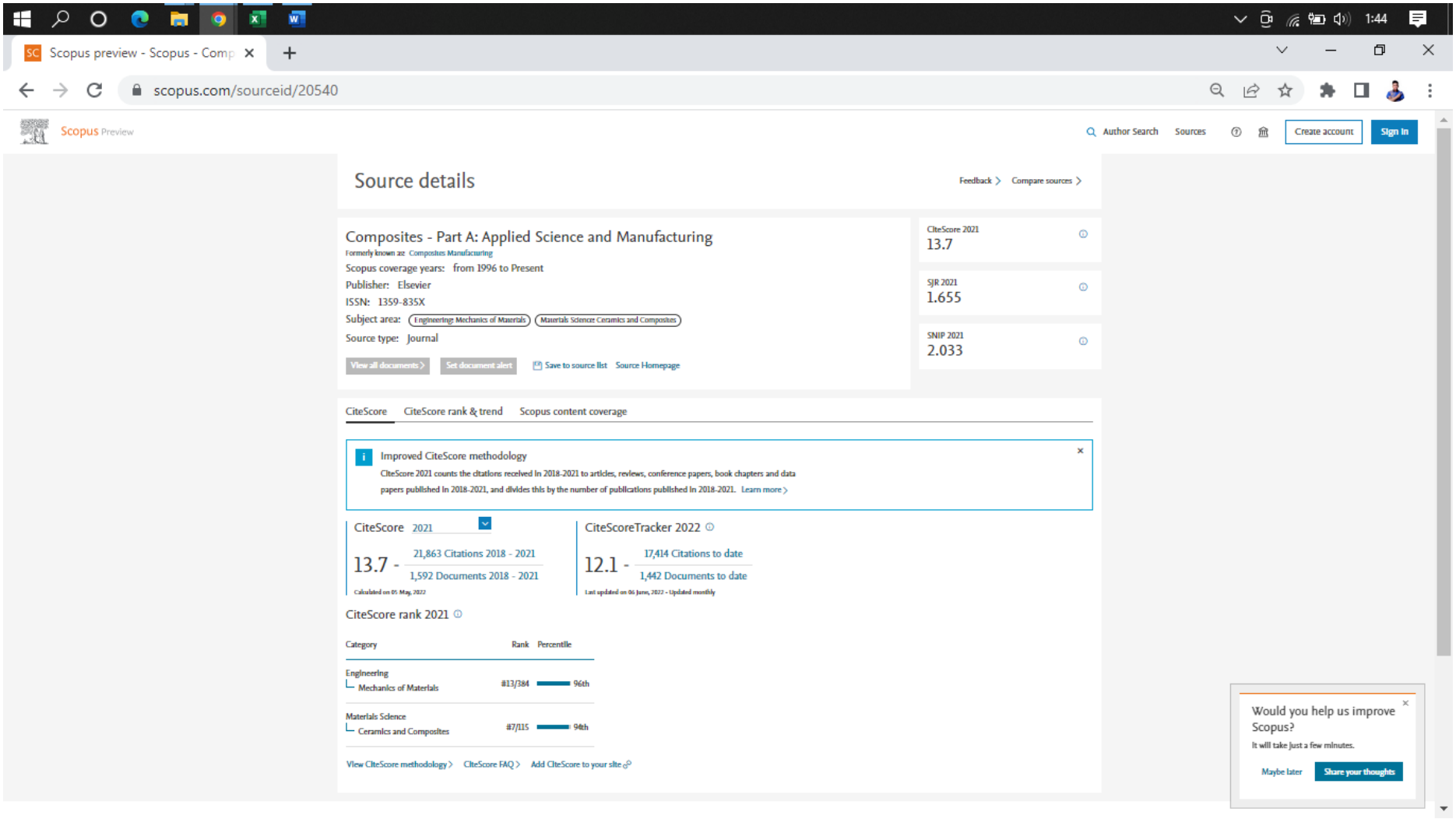
Scopus preview - Scopus - Comp
scopus.com/sourceid/20540
Scopus Preview
Author Search
Sources
Create account
Sign in
Source details
Feedback
Compare sources
Composites - Part A: Applied Science and Manufacturing
Formerly known as Composites Manufacturing
Scopus coverage years: from 1996 to Present
Publisher: Elsevier
ISSN: 1359-835X
Subject area: Engineering Mechanics of Materials
Materials Science Ceramics and Composites
Source type: Journal
View all documents
Set document alert
Save to source list
Source Homepage
CiteScore 2021
13.7
SJR 2021
1.655
SNIP 2021
2.033
CiteScore
CiteScore rank & trend
Scopus content coverage
Improved CiteScore methodology
CiteScore 2021 counts the citations received in 2018-2021 to articles, reviews, conference papers, book chapters and data papers published in 2018-2021, and divides this by the number of publications published in 2018-2021.
Learn more
CiteScore 2021
13.7 - 21,863 Citations 2018 - 2021 / 1,592 Documents 2018 - 2021
Calculated on 05 May, 2022
CiteScoreTracker 2022
12.1 - 17,414 Citations to date / 1,442 Documents to date
Last updated on 06 June, 2022 - Updated monthly
CiteScore rank 2021
Category
Rank
Percentile
Engineering
Mechanics of Materials
#13/384
96th
Materials Science
Ceramics and Composites
#7/115
94th
View CiteScore methodology
CiteScore FAQ
Add CiteScore to your site
Would you help us improve Scopus?
It will take just a few minutes.
Maybe later
Share your thoughts

Composites: Part A 143 (2021) 106273

Contents lists available at ScienceDirect

Composites Part A

journal homepage: www.elsevier.com/locate/compositesa

Biobased PLA/sugarcane bagasse fiber composites: Effect of fiber characteristics and interfacial adhesion on properties

András Bartos [a,b,*], Kristóf Nagy [a,b], Juliana Anggono [c], Antoni [d], Hariyati Purwaningsih [e], János Móczó [a,b], Béla Pukánszky [a,b]

[a] Laboratory of Plastics and Rubber Technology, Department of Physical Chemistry and Materials Science, Budapest University of Technology and Economics, H-1521 Budapest, P.O. Box 91, Hungary
[b] Institute of Materials and Environmental Chemistry, Research Centre for Natural Sciences, Eötvös Loránd Research Network, H-1519 Budapest, P.O. Box 286, Hungary
[c] Department of Mechanical Engineering, Petra Christian University, Jalan Siwalankerto 121-131, Surabaya 60236, Indonesia
[d] Civil Engineering Department, Petra Christian University, Jalan Siwalankerto 121-131, Surabaya 60236, Indonesia
[e] Materials and Metallurgical Engineering Department, Sepuluh Nopember Institute of Technology, Jalan Raya ITS Keputih Sukolilo, Surabaya 60111, Indonesia

ARTICLE INFO

Keywords:
A: biocomposite
B: adhesion
D: acoustic emission
E: injection moulding

ABSTRACT

PLA/sugarcane bagasse fiber composites were prepared by injection molding from two fractions of fibers with different fiber characteristics, which were determined before and after processing. Interfacial adhesion was modified by a maleated PLA coupling agent. The mechanical properties of the composites were characterized by tensile and impact testing, while local deformation processes by acoustic emission testing and microscopy. The results showed that considerable attrition takes place during melt processing in both the length and diameter of the fibers. The originally different batches of short and long fibers have similar dimensions after processing. Interfacial adhesion between PLA and bagasse is inherently good, thus coupling does not improve properties. Shear yielding and fiber fracture consume sufficiently energy to increase the impact resistance. Sugarcane bagasse fibers considerably increase the stiffness of PLA, result in almost constant tensile strength and increase impact resistance yielding a material with reasonable combination of properties for structural applications.

1. Introduction

Depleting fossil fuel resources and increasing environmental awareness of both the public and the industry increased the interest in raw materials derived from renewable resources. Polymers are versatile materials, which are used in a large number of applications in all areas of life. Their property profile can be extended even further by modification, stiffness, and strength can be increased by fiber reinforcement [1–3], fracture resistance by impact modification [4,5], flexibility and deformability by plasticization [6,7], etc. Fiber-reinforced composites are usually applied in structural applications mainly in the construction and automotive industry [8,9], but also in many other areas [1]. Completely biobased composites can be prepared from biopolymers and wood flour or other natural fibers [10–12]. Such composites compete successfully with traditional glass or carbon fiber reinforced commodity polymers and they are used more and more extensively for the production of automotive interior parts as door panels, trimming, sidings, hat racks, etc. [13,14].

However, wood and natural fiber reinforced biocomposites have several drawbacks as well [15]. The most frequently used matrix for such composites is poly(lactic acid) (PLA) produced in relatively large quantities and at a reasonable price. The properties of PLA are quite advantageous, certain types have relatively large stiffness (3 GPa) and strength (55 MPa), which compete with the similar properties of engineering thermoplastics. However, PLA is sensitive to water during processing [16], its physical ageing is fast leading to brittleness [17,18], and its deformability, as well as impact resistance, is small [19]. Similarly, natural fibers also have their disadvantages. Their properties depend on the source of the fiber, but also on climate changes and the period of the harvest. They absorb water leading to dimensional changes, they are sensitive to heat during processing, and the adhesion of the fibers to polymers is often quite poor [20,21].

In order to compensate for these disadvantages, numerous attempts are made to find the right combination of fiber and matrix polymer, and/

* Corresponding author at: Laboratory of Plastics and Rubber Technology, Department of Physical Chemistry and Materials Science, Budapest University of Technology and Economics, H-1521 Budapest, P.O. Box 91, Hungary.
E-mail address: bartos.andras@vbk.bme.hu (A. Bartos).

https://doi.org/10.1016/j.compositesa.2021.106273
Received 5 August 2020; Received in revised form 27 December 2020; Accepted 29 December 2020
Available online 7 January 2021

or to modify the components in various ways, or improve interfacial adhesion by coupling. Wood and other natural fibers were added to PLA as reinforcement earlier and the form of the reinforcement (particle [11,22–24], fiber [25–27] or mat [28]), as well as particle characteristics, changed in a wide range in published studies. Similarly, the characteristics of the fibers were modified by alkali treatment [26,29–31] and numerous surface modification techniques were used to improve interfacial adhesion between the fiber and the PLA from surfactants [32,33] to various small [11,26,29,30] and large molecular weight coupling agents [34,35]. The property combinations achieved cover a wide range, but the ever-increasing drive of the industry towards materials with better properties always allows room for further improvement.

One possible reinforcement for plastics is sugarcane bagasse fiber. It is a cheap, natural raw material obtained from local sources. Bagasse fibers are burned in the technology to produce sugar, but their value-added application would be beneficial for the countries producing it. The fiber can be homogenized directly with polymer matrices using an efficient processing technique like extrusion or injection molding. Several papers were published on polypropylene/sugarcane bagasse composites [36–39] and more recently on materials prepared with PLA matrix [40–44] as well. Some of the publications investigate interfacial interactions between the components. Khoo and Chow [42] observed voids between the matrix and the bagasse at the interface indicating weak adhesion. Hong et al. [40] studied the effect of different treatments (alkaline, silane and the combination of the two) on the structure and properties of PLA/bagasse fiber composites. They found that untreated and alkali-treated fibers were pulled-out from the matrix but the silane and the combined treatment improved interfacial adhesion, thus the number of fiber breakage increased considerably. Suryanegara et al. [44] observed that the tensile strength of PLA based composites decreases with increasing bagasse content and explained the phenomenon with poor adhesion as well as the formation of voids which result in inefficient stress transfer. In the papers cited above most of the conclusions about interfacial adhesion were drawn from the observation of SEM micrographs and they contradict our previous results indicating strong adhesion between PLA and natural fibers [12].

In accordance with the general tendency of going green and using local resources, the goal of our study was to prepare fully biodegradable biobased composites from PLA and sugarcane bagasse fibers and explore the property profile of the materials produced. The fibers were obtained from a local sugar mill in Indonesia and they were separated into two fractions with different sizes in order to study the effect of fiber characteristics on composite properties. The injection molded specimens prepared from the composites contained the fibers in various amounts and a functionalized, maleic anhydride modified PLA was used as coupling agent to improve interfacial adhesion. The material was characterized by standard tensile and impact measurements and local deformation processes were followed by acoustic emission testing in order to facilitate the interpretation of the effect of the studied variables (composition, fiber characteristics, adhesion) on composite properties. The practical relevance of the results is also discussed briefly at the end of the paper.

2. Experimental

2.1. Materials

The bagasse fibers were obtained directly from the sugar mill (Candi Baru Sugar Factory, Sidoarjo, Indonesia). They were washed with ethanol, dried, cut and sieved. The fibers were separated into two, a long and a short, fractions in order to study the effect of fiber characteristics on composite properties. The long fraction was obtained by combining fibers collected from the 0.8 mm (20 mesh) and 0.35 mm (45 mesh) sieves, and the short fraction consisted of the fibers passing through all sieves. The dimensions of the fibers were determined by digital optical microscopy before and after processing; the characteristics are compiled in Table 1. The density of the fibers was determined by using a pycnometer; the value obtained was 1.2 g/cm^3.

The PLA used as matrix was obtained from NatureWorks (Minnetonka, MN, USA). The selected grade (Ingeo 4032D, $M_n = 88500$ g/mol and $M_w/M_n = 1.8$) is recommended for extrusion. The polymer (<2% D isomer) has a density of 1.24 g/cm^3, while its melt flow rate (MFR) is 3,9 g/10 min at 190 °C and 2.16 kg load. The functionalized PLA coupling agent (MAPLA) was produced in our laboratory according to the method developed earlier [34]. The PLA used in the grafting reaction was the Ingeo 3251D grade obtained from NatureWorks (Minnetonka, MN, USA). Its MFR was 35 g/10 min at 190 °C and 2.16 kg load. PLA was dried for 4 h at 100 °C and 150 mbar pressure. 4 g maleic anhydride (Merck KGaA, Darmstadt, Germany) was dissolved in 20 ml acetone (Molar Chemicals Kft, Halásztelek, Hungary) and then 4 g Luperox 101 (Arkema, Colombes, France) peroxide was added to the solution. The latter was poured onto 200 g PLA and homogenized in a plastic bag. The granules were placed into an air circulating oven (Memmert UF450, Memmert GmbH, Schwabach, Germany) for 5 min at 80 °C to evaporate the solvent. Reactive processing was carried out using a Brabender Lab-Station (Brabender GmbH, Duisburg, Germany) single screw extruder with the temperature profile of 175-180-185-190 °C at 12 rpm. The grafted polymer was characterized by NMR spectroscopy (Varian NMR System, Agilent Technologies, Inc., Santa Clara, CA, USA), but was not purified; it was used as obtained in the reaction.

2.2. Sample preparation

Before processing, the fibers were dried for 4 h at 105 °C (Memmert UF450, Memmert GmbH, Schwabach, Germany), in order to eliminate the moisture absorbed during standing in the laboratory. The PLA and the coupling agent were also dried in a vacuum oven (Memmert VO101, Memmert GmbH, Schwabach, Germany) at 100 °C and 150 mbar pressure for 4 h. The fibers and the polymer were thoroughly mixed in a plastic bag and then homogenized in a twin-screw compounder (Brabender DSK 42/7, Brabender GmbH, Duisburg, Germany) at the set temperatures of 170-180-185-190 °C and 40 rpm. The fiber content of the composites changed from 0 to 30 wt% in 5 wt% steps. The amount of the coupling agent was always 10% calculated for the reinforcement and it was added at the expense of the matrix polymer. Weight percentages were used for sample preparation, but mechanical properties depend on the volume fraction of the reinforcement. This latter was calculated by using the density of the components (see above). The granulated composites were injection molded into standard (ISO 527 1A) tensile bars of 4 mm thickness using a Demag IntElect 50/330-100 (Demag Ergotech GmbH, Schwaig, Germany) machine. Processing parameters were 40-170-180-185-190 °C set temperature, 800–1200 bar injection pressure depending on fiber content, 50 mm/s injection speed, 650–800 holding pressure, 15 s holding time, and 45 s cooling time. The temperature of the mold was set to 20 °C. The specimens were stored at ambient temperature (23 °C, 50% RH) for a week before further testing.

Table 1
Dimensions of the bagasse fibers used before and after processing.

Fiber	Coupling	Processing	Length (μm)	Diameter (μm)	Aspect ratio
Short	–	before	815 ± 626	221 ± 120	3.96
	–	after	468 ± 253	201 ± 100	2.73
	+	after	592 ± 330	234 ± 109	2.65
Long	–	before	2845 ± 1260	716 ± 385	5.09
	–	after	729 ± 320	271 ± 128	2.98
	+	after	746 ± 410	278 ± 155	2.96

2.3. Characterization

Fiber characteristics were determined by digital optical microscopy (Keyence VHX 500, Keyence Co., Osaka, Japan). The fibers were evenly distributed on a glass plate for the determination. The dimensions of 6–700 fibers were measured both before and after processing. In order to determine fiber dimensions after processing, composite samples were put into boiling tetrahydrofuran (Molar Chemicals Kft., Halásztelek, Hungary) for 4 h to dissolve the polymer, and then the fibers were sieved and dried. Fiber dimensions were determined using the ImagePro 10 (Media Cybernetics, Inc., Rockville, MD, USA) software. The mechanical properties of the composites were characterized by tensile and impact testing. Tensile tests were carried out using an Instron 5566 (Instron, Norwood, MA, USA) universal testing machine according to the ISO 527 1A standard with a gauge length of 115 mm and 5 mm/min crosshead speed using a 10 kN load cell. Elongation was measured by a strain gauge and the results were used for the calculation of modulus. Five parallel measurements were done at each composition. Modulus, tensile strength and elongation-at-break were derived from recorded stress vs. strain traces. Local deformation processes were followed by acoustic emission testing (AE) using a Sensophone AED 404 (Geréb és Társa Ltd., Budapest, Hungary) apparatus. A single a11 resonance detector with the resonance frequency of 150 kHz was attached to the center of the specimen. The threshold level of detection was set to 25 dB. Impact resistance was characterized by the notched Charpy impact strength (Zwick Pendulum Impact Tester HIT5.5P, Zwick Roell Group, Ulm, Germany), which was determined according to the ISO 179 standard with 2 mm notch depth at 23 °C, using a 0.5 J hammer. Seven parallel measurements were carried out on each material. Instrumented impact testing was done by using the same equipment with a 4 J hammer. Dynamic effects were suppressed with mechanical damping achieved with the application of a silicon rubber strip of 1 mm thickness. The appearance of broken surfaces was studied by scanning electron microscopy (Jeol JSM 6380 LA, Jeol Ltd., Tokyo, Japan). Micrographs were recorded on fracture surfaces created during tensile and fracture testing, respectively, at the accelerating voltage of 15 kV. Before recording the micrographs, the surfaces were sputtered with gold for 35 s using a Jeol Fine Coater (Jeol Ltd., Tokyo, Japan) apparatus.

3. Results and discussion

The results are discussed in several sections. First, the dimensions of the two batches of fibers used as reinforcement are shown together with the effect of processing on them. Subsequently, mechanical properties are presented followed by the analysis of local deformation processes and their possible impact on properties. The results are discussed in the last section of the paper together with comments on relevance for practice.

3.1. Fiber characteristics, the effect of processing

The dimensions of the reinforcing fibers are very important for composite properties since the orientation of the fibers, as well as their aspect ratio, determine the extent of reinforcement. As mentioned in the experimental part, two fractions of the bagasse fibers were separated, which had different dimensions. However, stiff fibers often break up during the melt processing of composite materials and the extent of attrition determines fiber length and aspect ratio in them. Accordingly, the length, diameter and aspect ratio of the fibers were determined before and after processing and the results are listed in Table 1. Both the length and the diameter of the fibers differed significantly before processing; both dimensions of the long fibers were about three-four times larger than those of their shorter counterparts.

Processing led to considerable attrition in both cases, but the change was larger for the long fibers than for the short ones that is not very surprising. It is interesting to note, though, that not only the length, but also the diameter of the fibers decreased considerably for the long fibers; the diameter of the short fibers remained practically the same as before processing. The decrease of diameter indicates that the transverse strength of the fibers is not very large and they split easily along their axis. Although fiber dimensions still differ somewhat for the long and short fibers, but the differences are much smaller than before processing. The relatively small differences in fiber dimensions forecast similar reinforcing effect for the two fractions of the fibers.

3.2. Mechanical properties

Although PLA is used in large quantities in the packaging industry, it is often applied also as structural material. The stiffness, strength and often the impact resistance are the most important properties for such materials. The stiffness of the PLA/bagasse fiber composites is plotted in Fig. 1 against composition. Increasing fiber content results in significant reinforcement, the stiffness of the material almost doubles in the composition range used in this study. Long fibers have slightly larger reinforcing effect than the shorter ones, but the difference is not very large in accordance with the small deviation in size and especially in aspect ratio, as shown by Table 1 and discussed above. Coupling, i.e. the use of maleated PLA does not have practically any effect, but this is in accordance with our previous experience showing that interfacial adhesion has only a slight effect on stiffness [34].

The strength of the composites is plotted against composition in Fig. 2. Strength does not change much with composition that is beneficial for the application of these composites as structural material. Short fibers reinforce the polymer somewhat less than the longer ones, but in view of the fiber characteristics of the two fractions this difference agrees well with the expectations. It is somewhat more surprising that coupling does not have any effect on strength either. The strength of PP composites, for example, decreases drastically with increasing fiber content in the absence of coupling [45,46]. The very small influence of coupling on strength can be explained with our earlier results obtained on PLA/wood composites showing that, contrary to numerous literature references [22,23,25,27,40,42,44], interfacial adhesion between PLA and lignocellulosic reinforcements is quite strong [12]. Accordingly, improved interfacial adhesion due to the presence of MAPLA may prevent the debonding of a few fibers with large size and especially with large diameter, but otherwise it has a small effect, and other processes

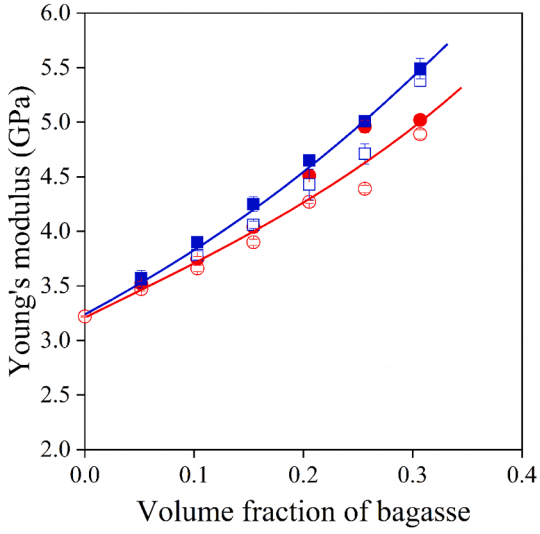

Fig. 1. Effect of composition, fiber characteristics and interfacial adhesion on the stiffness of PLA/bagasse fiber composites. Symbols: (○) short, no MAPLA, (●) short with MAPLA, (□) long, no MAPLA, (■) long, MAPLA. (For interpretation of the references to color in this figure legend, the reader is referred to the web version of this article.)

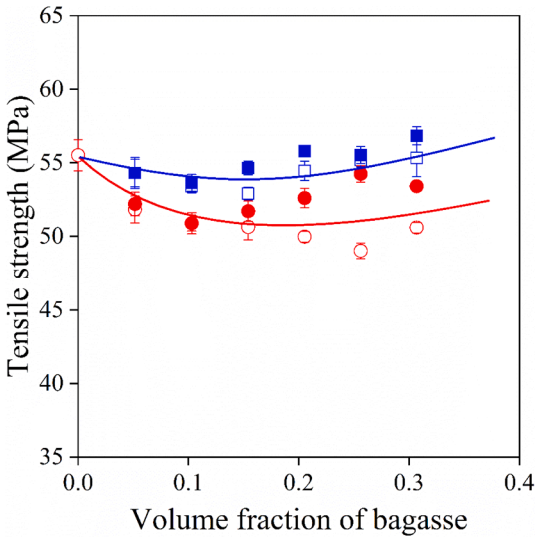

Fig. 2. Tensile strength of PLA/bagasse fiber composites plotted against fiber content. The influence of fiber dimensions and coupling. Symbols are the same as in Fig. 1. (For interpretation of the references to color in this figure legend, the reader is referred to the web version of this article.)

than debonding may also play a role in the determination of composite properties.

As expected, the deformability of the composites is small, elongation-at-break changes from 6% of the neat polymer to about 1.5% for the composite containing 30 wt% bagasse fibers (not shown). None of the variables studied, i.e. fiber dimensions or interfacial adhesion, influences deformability practically at all, at the same fiber content the composites have very similar elongations. Small deformability forecasts brittle fracture and poor impact resistance.

The fracture resistance of the PLA/bagasse fiber composites studied is presented in Fig. 3 as a function of composition. Contrary to the prediction mentioned above, impact strength increases with fiber content. The impact resistance of composites containing the short fibers is somewhat smaller and goes through a maximum, while it approaches a plateau for the composites prepared with the long fibers. Since the stiffness of the composites increased considerably with increasing fiber content, and usually an inverse correlation exists between stiffness and

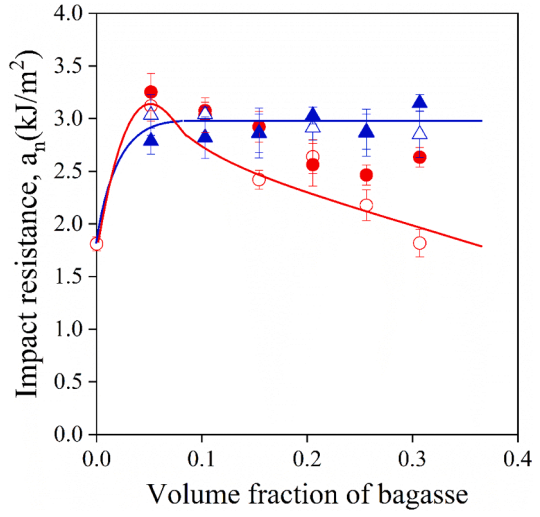

Fig. 3. Increase of the notched impact resistance of PLA/bagasse fiber composites with increasing fiber content. Symbols are the same as in Fig. 1. (For interpretation of the references to color in this figure legend, the reader is referred to the web version of this article.)

impact resistance for most structural materials, the observed phenomenon is rather surprising and needs further consideration and explanation. One reason for the increase might be the fact that bagasse fibers initiate local deformation processes, which consume energy and improve impact resistance.

3.3. Deformation and failure processes

PLA/bagasse fiber composites are heterogeneous materials with components having considerably different elastic properties. Different mechanical characteristics lead to the development of stress concentrations, which during deformation initiate local deformation processes around the heterogeneities, i.e. around the fibers, in this case. In composites containing fibers with large diameter several local deformation processes may take place including the debonding of the fibers from the matrix polymer, fiber pullout or fracture and occasionally also the shear yielding of the matrix. Some of these processes (debonding, fracture) can be followed by acoustic emission testing. The piezoelectric sensor placed on the specimens can detect local processes during tensile testing. The result of such a test is presented in Fig. 4. The small circles in the figure indicate individual acoustic events the height of which is proportional to the amplitude of the signal. Since the evaluation of individual signals is difficult, we plotted their cumulative number, i.e. the sum of signals detected up to a certain elongation (right axis) as well. The stress vs. elongation correlation (left axis) is also presented in the figure for reference. The result shown for the composite containing 5 wt% of the long fibers with MAPLA is typical, acoustic emission measurements yielded very similar results for all composites.

We can see that signals start to appear above a certain elongation, i.e. there is an initiation deformation or stress of the process, and signals are detected up to the end of the test. A closer scrutiny of the cumulative number of signal vs. elongation correlation indicates that it can be divided into two sections, i.e. two processes take place during deformation. Characteristic deformations and stresses can be assigned to these processes in the way indicated in Fig. 4. The composition dependence of the characteristic stresses determined from the acoustic emission test is presented in Fig. 5. We can see that the two processes have very different initiation stresses, that of the first step is below 20 MPa, while the second is at around 40 MPa. Based on the acoustic emission

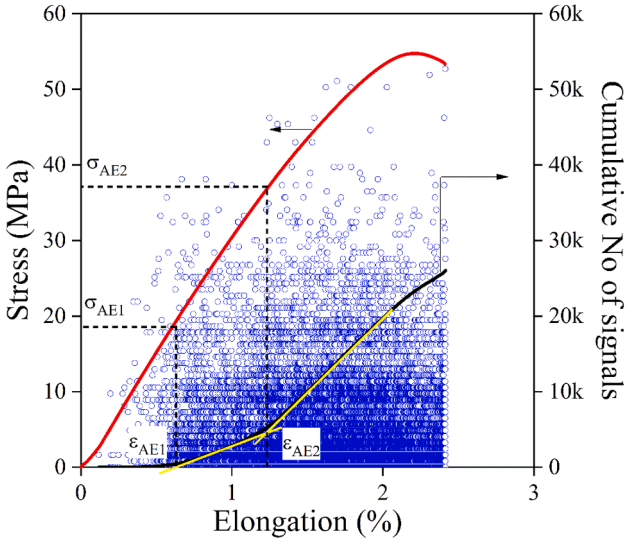

Fig. 4. The results of the acoustic emission testing of a PLA/bagasse fiber composite. Composition: 5 wt% of long bagasse fiber with MAPLA coupling agent. Symbols: (○) individual acoustic signals, full lines are the stress vs. elongation (left axis) and the cumulative number of signal vs. elongation (right axis) correlations. (For interpretation of the references to color in this figure legend, the reader is referred to the web version of this article.)

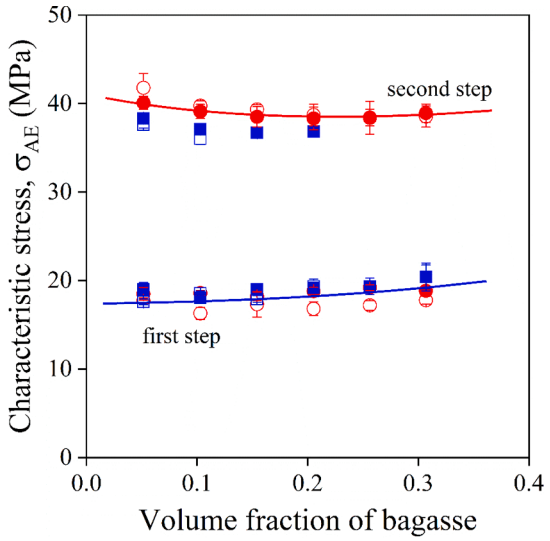

Fig. 5. Composition dependence of the characteristic stress of the local deformation processes detected by acoustic emission testing. The symbols are the same as in Fig. 1. (For interpretation of the references to color in this figure legend, the reader is referred to the web version of this article.)

measurements we can only speculate about these two processes, but earlier experience showed that debonding is initiated at smaller stresses, while the second process characterized by larger initiation stress is usually fiber pullout or fiber fracture. Since the analysis of fiber characteristics before and after processing showed the relatively facile fracture of the fibers also in the transverse direction, we may safely assume that fiber fracture occurs also during mechanical deformation.

SEM micrographs recorded on the fracture surfaces of the specimens may offer further information about the local processes taking place during deformation. A few representative micrographs are presented in Fig. 6. The fracture of a large fiber can be observed in Fig. 6a recorded on a composite containing the short fibers without coupling. Besides the fracture of the long fiber, a closer inspection reveals the presence of fibers with smaller aspect ratio, and shows that they tend to debond from the matrix during deformation. Coupling, i.e. the presence of the MAPLA coupling agent, does not modify the processes taking place during deformation; Fig. 6b shows basically the same picture as the previous one, i.e. debonding and fiber fracture are the dominating local deformation processes. This observation confirms our previous conclusion about the small effect of coupling on composite properties. The study of a large number of micrographs indicated that besides these two processes, some shear yielding of the matrix also occurs at certain places. As Fig. 6c shows, yielding takes place mainly around fibers with small aspect ratio. All the above micrographs were recorded on composites prepared with the short fibers. For demonstration, we present a micrograph in Fig. 6d taken from the fracture surface of a composite containing the longer fiber. The micrograph delivers practically the same message as the previous ones (Fig. 6a and b), the small difference in fiber length does not change the local processes taking place during deformation.

Acoustic emission testing and the SEM study shows that three processes take place during the deformation of the PLA/bagasse fiber composites. Debonding does not consume much energy thus might not explain the increase in impact resistance, but yielding and fiber fracture might. The fact that considerable fiber fracture takes place is confirmed by the SEM micrographs, but it is further supported by Fig. 7. The characteristic stress of the second process detected by acoustic emission is plotted against fiber content and it is extrapolated to the volume fraction of 1. This approach which can be used only if adhesion is strong and fiber fracture is the dominating local deformation process was used earlier to determine the inherent strength of the fibers [47]. The similar

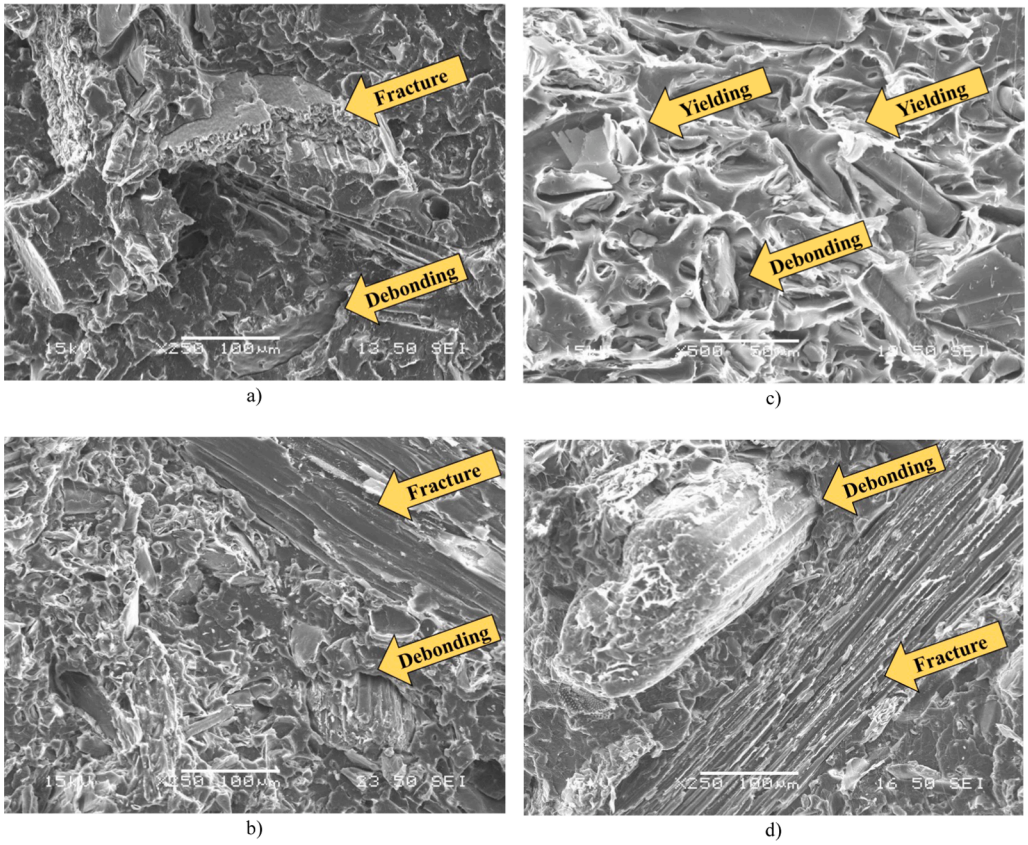

Fig. 6. SEM micrographs recorded on the fracture surface of PLA/bagasse fiber composites. The surfaces were created in tensile testing. Fiber content is always 20 wt%. Local processes are indicated by arrows in the micrographs. a) short fiber without MAPLA (fracture, debonding), b) short fiber with MAPLA (fracture, debonding), c) short fiber without MAPLA (debonding, shear yielding) d) long fiber without MAPLA (fracture debonding). (For interpretation of the references to color in this figure legend, the reader is referred to the web version of this article.)

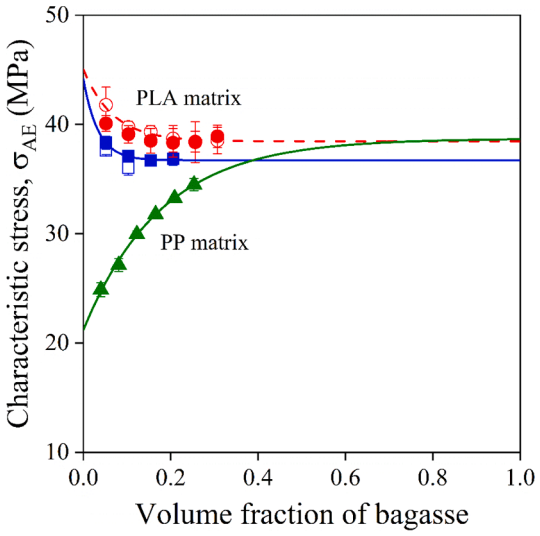

Fig. 7. Composition dependence of the characteristic stress determined during the acoustic emission testing of bagasse fiber composites. Determination of the inherent strength of the fibers [47]. Symbols are the same as in Fig. 1. Additional symbol: (▲) PP/bagasse fiber composite at good adhesion achieved with a maleated PP (MAPP) coupling agent. (For interpretation of the references to color in this figure legend, the reader is referred to the web version of this article.)

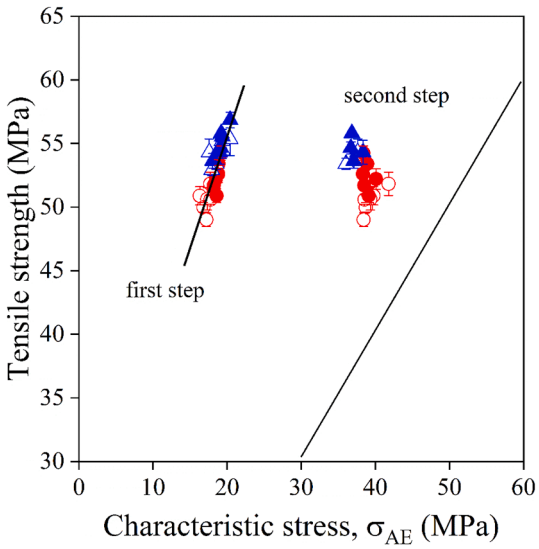

Fig. 8. Correlation between the characteristic stresses of local processes determined by acoustic emission testing and the tensile strength of PLA/bagasse fiber composites. Symbols are the same as in Fig. 1. (For interpretation of the references to color in this figure legend, the reader is referred to the web version of this article.)

correlation obtained for PP/bagasse fiber composites in the same way is also plotted as a reference. We can see that the correlations extrapolate to very similar values irrespectively of the matrix polymer. Larger fibers extrapolated to a smaller value, because the probability of flaws is larger in them thus their inherent strength is smaller as it was shown earlier for wood particles [47]. From these results we can draw the conclusion that fibers fracture during deformation, mainly parallel to their axis, and the process may contribute to energy absorption.

3.4. Discussion

The production of PLA composites suitable as structural material is rather challenging for several reasons. The stiffness of PLA is reasonable and it can be increased further by the addition of fibers. On the other hand, the physical ageing of this polymer is fast resulting in further increase in stiffness, but a drastic decrease of deformability [17]. The original elongation-at-break value of around 200% for freshly prepared samples decreases to a few percent in less than a week. Accordingly, the material fails in brittle fracture and impact resistance is usually not very large. The addition of stiff fibers to the already brittle polymer is expected to decrease fracture resistance even further.

In our case, however, impact resistance increased upon the addition of bagasse fibers and with increasing fiber content. The effect must result from local deformation processes, of which several takes place during the deformation of the specimen. Earlier experience showed that debonding does not consume much energy, but shear yielding initiated by it or fiber fracture do. Local deformation processes usually determine the macroscopic properties of composites. Close relationship has been shown earlier between one of the local processes and the strength of the composites [12,48]. Tensile strength is plotted against the characteristic stresses of the processes detected by acoustic emission testing in Fig. 8. Shear yielding does not give a signal, thus it cannot be detected in this way. The straight line drawn in the right side of the figure indicates identical characteristic stress and tensile strength, i.e. immediate failure upon the occurrence of the local process. Quite surprisingly, neither process leads to immediate failure. The initiation stress of the first, probably debonding, is much smaller than tensile strength. Failure follows not much after the second process, but not immediately. Accordingly, the second process may consume energy before failure thus increasing impact resistance. Obviously, the combination of parameters selected in this study leads to the preparation of composites with acceptable properties. Stiffness increases as expected, but local processes initiated by the fibers result in energy absorption and some increase in impact resistance. Good adhesion between the fibers and PLA leads to large strength even without coupling. The combination of these properties makes these composites good candidates for structural applications.

4. Conclusions

The determination of particle characteristics before and after processing showed that considerable attrition takes place during melt processing in both the length and diameter of the fibers. The reinforcement is fiber-like with small aspect ratio and the originally different batches of short and long fibers have similar particle characteristics after processing. The results also confirmed that the interfacial adhesion between PLA and lignocellulosic fibers is good, thus coupling is superfluous and does not improve properties. The analysis of local deformation processes by acoustic emission testing and microscopy showed that three local processes take place in the material during deformation: debonding, shear yielding and the fracture of the fibers. At least two of these processes, shear yielding and fracture, consume sufficiently energy to increase the impact resistance of the material. The modification of PLA with sugarcane bagasse fibers results in considerably increased stiffness, almost constant tensile strength and slightly increased impact resistance yielding a material with reasonable combination of properties for structural applications. Properties might be improved even further with the optimization of the dimensions of the bagasse fibers.

CRediT authorship contribution statement

András Bartos: Methodology, Investigation, Data curation, Writing - original draft, Writing - review & editing, Visualization. **Kristóf Nagy:** Investigation. **Juliana Anggono:** Conceptualization, Writing - review & editing. **Antoni:** Investigation, Resources. **Hariyati Purwaningsih:** Investigation, Resources. **János Móczó:** Conceptualization, Methodology, Data curation, Writing - original draft, Writing - review & editing. **Béla Pukánszky:** Conceptualization, Methodology, Writing - original

draft, Supervision.

Declaration of Competing Interest

The authors declare that they have no known competing financial interests or personal relationships that could have appeared to influence the work reported in this paper.

Acknowledgements

The National Research, Development and Innovation Fund of Hungary (OTKA K 120039 and FK 129270) is greatly acknowledged for the financial support of the research. We are also grateful to the Ministry of Research, Technology and Higher Education of the Republic of Indonesia for the research grant 002/SP2H/LT/MONO/L7/2019. The Candi Baru Sugar Factory, Indonesia is acknowledged for providing the sugarcane bagasse fibers.

Appendix A. Supplementary data

Supplementary data to this article can be found online at https://doi.org/10.1016/j.compositesa.2021.106273.

References

[1] Chu FP. Glass fiber–reinforced polypropylene. In: Karian H, editor. Handbook of polypropylene and polypropylene composites, revised and expanded. Boca Raton: CRC Press; 2003. p. 281–351.
[2] Zhang J, He W, Wu Y, Wang N, Chen X, Guo J. The evolution of morphology, crystallization and static and dynamic mechanical properties of long glass-fibre–reinforced polypropylene composites under thermo-oxidative ageing. J Thermoplast Compos 2019;32(4):544–57.
[3] Yin X, Yin Y, Feng Y, Zhang G, Wen Y. Preparation and characterization of carbon fiber/polypropylene composites via a tri-screw in-line compounding and injection molding. Adv Polym Tech 2018;37(8):3861–72.
[4] Jafari SH, Gupta AK. Impact strength and dynamic mechanical properties correlation in elastomer-modified polypropylene. J Appl Polym Sci 2000;78(5):962–71.
[5] Fasihi M, Mansouri H. Effect of rubber interparticle distance distribution on toughening behavior of thermoplastic polyolefin elastomer toughened polypropylene. J Appl Polym Sci 2016;133(40):44068.
[6] Kulinski Z, Piorkowska E, Gadzinowska K, Stasiak M. Plasticization of poly(L-lactide) with poly(propylene glycol). Biomacromolecules 2006;7(7):2128–35.
[7] Lemmouchi Y, Murariu M, Dos Santos AM, Amass AJ, Schacht E, Dubois P. Plasticization of poly(lactide) with blends of tributyl citrate and low molecular weight poly(D, L-lactide)-b-poly(ethylene glycol) copolymers. Eur Polym J 2009;45(10):2839–48.
[8] Flowers B. Automotive applications for polypropylene and polypropylene composites. In: Karian H, editor. Handbook of polypropylene and polypropylene composites, revised and expanded. Boca Raton: CRC Press; 2003. p. 578–86.
[9] Elliott ANA. Automotive applications of polymers II. Shrewsbury: Rapra Technology Limited; 1992.
[10] Müller P, Renner K, Móczó J, Fekete E, Pukánszky B. Thermoplastic starch/wood composites: Interfacial interactions and functional properties. Carbohyd Polym 2014;102(1):821–9.
[11] Faludi G, Dora G, Renner K, Móczó J, Pukánszky B. Improving interfacial adhesion in pla/wood biocomposites. Compos Sci Technol 2013;89:77–82.
[12] Faludi G, Dora G, Imre B, Renner K, Móczó J, Pukánszky B. PLA/lignocellulosic fiber composites: Particle characteristics, interfacial adhesion, and failure mechanism. J Appl Polym Sci 2014;131(4):39902.
[13] Rusu D, Boyer SAE, Lacrampe MF, Krawczak P. Bioplastics and vegetal fiber reinforced bioplastics for automotive applications. In: Pilla S, editor. Handbook of bioplastics and biocomposites engineering applications. Beverly: Scrivener Publishing LLC.; 2011. p. 397–449.
[14] Suddell BC, Evans WJ. Natural fiber composites in automotive applications. In: Mohanty AK, Mishra M, Drzal LT, editors. Natural fibers, biopolymers and biocomposites. Boca Raton: CRC Press; 2005. p. 231–59.
[15] Bledzki AK, Gassan J. Composites reinforced with cellulose based fibres. Prog Polym Sci 1999;24(2):221–74.
[16] Auras R, Harte B, Selke S. An overview of polylactides as packaging materials. Macromol Biosci 2004;4(9):835–64.
[17] Cui L, Imre B, Tátraaljai D, Pukánszky B. Physical ageing of poly(lactic acid): Factors and consequences for practice. Polymer 2020;186:122014.
[18] Müller P, Imre B, Bere J, Móczó J, Pukánszky B. Physical ageing and molecular mobility in PLA blends and composites. J Therm Anal Calorim 2015;122(3):1423–33.
[19] Coltelli M-B, Mallegni N, Rizzo S, Cinelli P, Lazzeri A. Improved impact properties in poly(lactic acid) (PLA) blends containing cellulose acetate (CA) prepared by reactive extrusion. Materials 2019;12(2):270.
[20] Rowell RM. Natural fibres: types and properties. In: Pickering KL, editor. Properties and performance of natural-fibre composites. Boca Raton: Woodhead Publishing; 2008. p. 3–66.
[21] Clemons C. Raw materials for wood-polymer composites. In: Oksman K, Sain M, editors. Wood-polymer composites. Boca Raton: CRC Press LLC; 2008. p. 1–22.
[22] Huda MS, Drzal LT, Misra M, Mohanty AK. Wood-fiber-reinforced poly(lactic acid) composites: Evaluation of the physicomechanical and morphological properties. J Appl Polym Sci 2006;102(5):4856–69.
[23] Mathew AP, Oksman K, Sain M. Mechanical properties of biodegradable composites from poly lactic acid (PLA) and microcrystalline cellulose (MCC). J Appl Polym Sci 2005;97(5):2014–25.
[24] Csizmadia R, Faludi G, Renner K, Móczó J, Pukánszky B. PLA/wood biocomposites: Improving composite strength by chemical treatment of the fibers. Compos Part A-Appl S 2013;53:46–53.
[25] Bax B, Müssig J. Impact and tensile properties of PLA/cordenka and PLA/flax composites. Compos Sci Technol 2008;68(7–8):1601–7.
[26] Huda MS, Drzal LT, Mohanty AK, Misra M. Effect of fiber surface-treatments on the properties of laminated biocomposites from poly(lactic acid) (PLA) and kenaf fibers. Compos Sci Technol 2008;68(2):424–32.
[27] Oksman K, Skrifvars M, Selin J-F. Natural fibres as reinforcement in polylactic acid (PLA) composites. Compos Sci Technol 2003;63(9):1317–24.
[28] Nishino T, Hirao K, Kotera M, Nakamae K, Inagaki H. Kenaf reinforced biodegradable composite. Compos Sci Technol 2003;63(9):1281–6.
[29] Ovlaque P, Foruzanmehr M, Elkoun S, Robert M. Milkweed floss fiber/PLA composites: effect of alkaline and epoxy-silanol surface modifications on their mechanical properties. Compos Interface 2020;27(5):495–513.
[30] Sawpan MA, Pickering KL, Fernyhough A. Improvement of mechanical performance of industrial hemp fibre reinforced polylactide biocomposites. Compos Part A-Appl S 2011;42(3):310–9.
[31] Orue A, Jauregi A, Unsuain U, Labidi J, Eceiza A, Arbelaiz A. The effect of alkaline and silane treatments on mechanical properties and breakage of sisal fibers and poly(lactic acid)/sisal fiber composites. Compos Part A-Appl S 2016;84:186–95.
[32] Wu YQ, Liu XM, Li XG. Effect of the interface control process of wood fiber/PLA on properties of composites. Adv Mater Res 2012;557–559:281–5.
[33] Zhang Q, Shi L, Nie J, Wang H, Yang D. Study on poly(lactic acid)/natural fibers composites. J Appl Polym Sci 2012;125:526–33.
[34] Csikós Á, Faludi G, Domján A, Renner K, Móczó J, Pukánszky B. Modification of interfacial adhesion with a functionalized polymer in PLA/wood composites. Eur Polym J 2015;68:592–600.
[35] Yu T, Jiang N, Li Y. Study on short ramie fiber/poly(lactic acid) composites compatibilized by maleic anhydride. Compos Part A-Appl S 2014;64:139–46.
[36] Luz SM, Gonçalves AR, Del'Arco AP. Mechanical behavior and microstructural analysis of sugarcane bagasse fibers reinforced polypropylene composites. Compos Part A-Appl S 2007;38(6):1455–61.
[37] Vázquez A, Domínguez VA, Kenny JM. Bagasse fiber-polypropylene based composites. J Thermoplast Compos 1999;12(6):477–97.
[38] Mulinari DR, Cipriano JdP, Capri MR, Brandão AT. Influence of surgarcane bagasse fibers with modified surface on polypropylene composites. J Nat Fibers 2018;15(2):174–82.
[39] Cerqueira EF, Baptista CARP, Mulinari DR. Mechanical behaviour of polypropylene reinforced sugarcane bagasse fibers composites. Procedia Eng 2011;10:2046–51.
[40] Hong H, Xiao R, Guo Q, Liu H, Zhang H. Quantitively characterizing the chemical composition of tailored bagasse fiber and its effect on the thermal and mechanical properties of polylactic acid-based composites. Polymers (Basel) 2019;11(10):1567.
[41] Lila MK, Shukla K, Komal UK, Singh I. Accelerated thermal ageing behaviour of bagasse fibers reinforced poly(lactic acid) based biocomposites. Compos Part B-Eng 2019;156:121–7.
[42] Khoo RZ, Chow WS. Mechanical and thermal properties of poly(lactic acid)/sugarcane bagasse fiber green composites. J Thermoplast Compos 2015;30(8):1091–102.
[43] Maryam A, Sahab H, Mehdi J, Ali A, Loya J. The influence of bio-fibers from different pulping processes on the pulp-polylactic acid composites (PPCs) properties from sugarcane bagasse. Nord Pulp Pap Res J 2019;34(3):239–49.
[44] Suryanegara L, Kurniawan YD, Syamani FA, Nurhamiyah Y. Mechanical properties of composites based on poly(lactic acid) and soda-treated sugarcane bagasse pulp. In: McLellan B, editor. Sustainable Future for Human Security: Society, Cities and Governance. Singapore: Springer Singapore; 2018. p. 277–85.
[45] Dányádi L, Janecska T, Szabó Z, Nagy G, Móczó J, Pukánszky B. Wood flour filled PP composites: Compatibilization and adhesion. Compos Sci Technol 2007;67(13):2838–46.
[46] Dányádi L, Renner K, Szabó Z, Nagy G, Móczó J, Pukánszky B. Wood flour filled PP composites: Adhesion, deformation, failure. Polym Advan Technol 2006;17(11–12):967–74.
[47] Faludi G, Link Z, Renner K, Móczó J, Pukánszky B. Factors determining the performance of thermoplastic polymer/wood composites; the limiting role of fiber fracture. Mater Des 2014;61:203–10.
[48] Renner K, Kenyó C, Móczó J, Pukánszky B. Micromechanical deformation processes in PP/wood composites: Particle characteristics, adhesion, mechanisms. Compos Part A-Appl S 2010;41(11):1653–61.